CALIBRATION OF THE TAGGED PHOTON BEAM:

NORMALIZATION METHODS, SHOWER COUNTER AND PAIR SPECTROMETER

Daniel I. Sober
The Catholic University of America
Washington, DC 20064

9 July 1992

This note was presented for discussion at the April 3, 1992 meeting of the Hall B TAC. It is very preliminary, and contains opinions which are solely those of the author.

1. INTRODUCTION

It is assumed that the tagged photon system will make use of two calibration devices: a total absorption shower counter (TASC) which will be inserted into the photon beam as needed, and a pair spectrometer (PS) which will reside in the downstream alcove leading to the beam dump. This note tries to make explicit the benefits of each of these devices, and discuss some of their properties.

There are at least three separate types of information which can come from these systems: absolute photon flux normalization, time calibration, and relative luminosity monitoring. These will be discussed in turn in Section 2. In Section 3, a design for the pair spectrometer is proposed, and some conclusions and questions are discussed in Section 4.

2. CALIBRATION

2.1 Calibration Runs

In order to calculate a cross section, we must know the number of incident photons n_i in energy bin i in a data run. The information needed to calculate n_i requires that three types of special calibration runs are performed for each incident energy and photon beam collimator. The CLAS target must be removed for these runs:

A. tagger + TASC (reduced beam rate)
B. tagger + pair spectrometer (same rate as A)
C. tagger + pair spectrometer (full rate)

Some of the properties of the triggers for these runs are summarized in Figure 1.

For runs of type A, a total-absorption shower counter (TASC) is placed in the photon beam. Although good energy resolution is not needed, the TASC must have ≈100% efficiency for photons down to ≈200 MeV. This requirement probably precludes using a lead-scintillator sandwich for this purpose. A lead-glass counter of length 10-12 radiation lengths and transverse size ≈15-20 cm should be adequate if it can be placed not too far downstream of the CLAS, since the maximum collimated photon beam size on the CLAS target should never exceed ≈6-8 cm.

The tagger information (E-counter and T-counter times) is recorded whenever a trigger is received from the TASC. There is a scaler for each T-counter, and for a "master OR" of T-counters, just as in the data runs.

Because an in-beam counter will certainly be rate-limited at much less than 3×10^7 photons/second, the TASC runs will be performed at reduced rate, probably $\approx 5 \times 10^5\ s^{-1}$. If events cannot be recorded at this rate, then rate division (i.e. prescaling the triggers) can be used.

The TASC can also be used to provide a common TDC STOP signal to calibrate the relative timing of the T and E counters. This will be discussed further in Section 2.3.

In order to check the deadtime corrections to the tagger electronics, we need an unbiased trigger from a detector which can operate at both the full beam rate of the data runs and the reduced beam rate of the TASC runs. A pair spectrometer with a thin (≈.01 radiation length) radiator, located in the beam dump alcove, has been proposed as the best solution. To be useful, the pair spectrometer must have a relatively flat acceptance for photons of all tagged energies ($0.2\ E_0$ to $0.95\ E_0$), and an aperture which accepts the entire collimated photon beam. The pair spectrometer is discussed in detail in Section 3.

2.2 Photon Flux Normalization

The calculation of a cross section requires the number of on-target incident photons n_i in energy bin i in a data run. This number can be obtained in various ways. Two possibilities are listed here. Method 1 is based on the T-counter scalers, and Method 2 depends on recording tagger data for randomly-selected tag events.

(Method 1)

$$n_i = N_{\gamma j} \times n_i^{TASC}(cal)/N_j(cal) \times (\epsilon_{TASC})_i \times (\eta_{DT})_i \tag{1}$$

where

N_j = number of scaled events in T-counter T_j (which overlaps E-counter E_{2i}),

$N_j(cal)$ = number of scaled events in the same T-counter in the type-A calibration run,

$n_i^{TASC}(cal)$ = number of photons in bin i associated with photons in the TASC in the type-A calibration run,

ϵ_{TASC} = efficiency of the TASC at the appropriate photon energy (presumably close to unity), and

η_{DT} = deadtime correction factor to account for rate-dependent differences in the electronics at the rates of the data and calibration runs.

The pair spectrometer calibration runs (types B and C above) provide the deadtime correction factor:

$$(\eta_{DT})_i = (n_i(PS\text{-}high)/N_j(PS\text{-}high)) \div (n_i(PS\text{-}low)/N_j(PS\text{-}low)) \qquad (2)$$

where the n_i are the number of tags in bin i in coincidence with the pair spectrometer, and the labels "PS-high" and "PS-low" refer to runs of type C and B respectively.

(Method 2)

Here, in the type-A calibration run, tagger data acquisition is triggered by the "master OR" of the T-counters, and the presence or absence of a photon in the TASC is determined by examining the TASC TDC channel. In the data run, a "sampled" spectrum is accumulated alongside the CLAS-trigger events by triggerin the tagger data acquisition by rate division of the master OR.

$$n_i = M_S \times n^S_i \times n^{TASC}_i(cal)/n_i(cal) \times (\epsilon_{TASC})_i \times (\eta_{DT})_i \qquad (3)$$

where

M_S = "sampling" or rate-division factor used to count down the tagger "master OR" during data run

n^S_i = number of events in energy bin i in the "sampled" spectrum

$n^{TASC}_i(cal)$ = number of photons in bin i associated with photons in the TASC in the type-A calibration run,

$n_i(cal)$ = number of photons in bin i in the type-A calibration run, whether or not associated with events in the TASC.

ϵ_{TASC} and η_{DT} are defined as above. The deadtime factor is now

$$(\eta_{DT})_i = (n^S_i(PS\text{-}high)/n^{PS}_i(PS\text{-}high)) \div (n^S_i(PS\text{-}low)/n^{PS}_i(PS\text{-}low)) \qquad (4)$$

where n^{PS}_i is the number of events in bin i of the spectrum triggered by the pair spectrometer; the labels "PS-high" and "PS-low" again refer to runs of types C and B respectively.

The above relationships for Methods 1 and 2 are summarized in Figures 2 and 3. The advantage of Method 1 is that it requires less data acquisition for the same statistics, as there will always be many more events in the T-counter scalers than can be analyzed. The advantage of Method 2 is that it effectively requires a coincidence between the T and E counters, and thus is less susceptible to background than a singles scaler.

2.3 Time Calibration

Making use of the 2 ns RF bunch structure of the Hall B beam to minimize accidentals in the final data set will require careful time alignment of the T- and E-counters. This can be done most easily by sending a common TDC stop signal from an in-beam counter, such as the TASC described above.

It is not clear, however, that the lead-glass counter envisioned for the flux calibration will have good enough time resolution for this purpose. Since the Cherenkov light travels forward and the shower propagates appreciably faster than the light ($n \approx 1.6$-1.8), the leading edge of the PMT signal will be dominated by the large-depth "tail" of the shower, which is very energy-dependent and exhibits large straggling at low energies. Constant-fraction discrimination is also problematic because of PMT saturation and the energy dependence of the shower shape, and the variation in the position of the shower onset introduces fluctuations at all energies.

A shift of 1 radiation length ($\approx$3 cm) in the source of the light introduces a timing shift of order (3 cm)(1 ns/30 cm)(1.8-1.0) $\approx$ 0.1 ns, so perhaps these effects are not really serious, but they are not negligible and should be estimated using EGS or similar calculations. Such calculations will also allow a determination of the optimum refractive index and radiation length for the TASC.

If the lead glass counter proves not to provide good enough stability for time calibration, another option is to use a single-plane converter plus scintillator in the beam, with leading-edge discrimination. The lack of uniformity of efficiency is not a problem in this case.

2.4 Pair Spectrometer as a Relative Luminosity Monitor

A second use for the pair spectrometer is as a relative luminosity monitor during data runs. In this mode, no pair conversion target is needed, as the typical CLAS target will produce far more pairs than we want:

CLAS target	pairs/10^7 photons
1 g/cm^2 of $H_2 \approx 0.016$ R.L.	1.2×10^5
1 g/cm^2 of C ≈ 0.023 R.L.	1.8×10^5

(One could imagine sweeping these CLAS-produced pairs out of the photon beam in order to make the pair spectrometer data comparable to the calibration runs, but this would require **another** large magnet suspended in an impossible position. We leave this possibility for the consideration of more creative minds.)

The pair spectrometer triggers must normally be pre-scaled by a large factor, with (say) every 512th PS event triggering the data acquisition system. The acceptance of the pair spectrometer will be very energy-dependent and target-dependent: because of multiple scattering in the CLAS target, proportionately more of the low-energy e^+ and e^- will miss the magnet aperture. However, for a given incident energy E_0 and a given target the pair spectrometer can provide a stable relative normalization of the tagger channels which can be checked periodically to look for failures and shifts in efficiency.

3. PAIR SPECTROMETER

3.1 Design Criteria

1. The pair spectrometer must detect the e^+ and e^- in coincidence in order to be free of background events.

2. The pair spectrometer resides in the downstream alcove.

3. The magnet aperture must be larger than the size of the collimated photon beam when it reaches the alcove.

   The largest collimated photon beam at the CLAS target will be of diameter ≈6-8 cm. At the alcove, this will have expanded to ≈(8cm)(6+15+15m)/(6+15m) ≈ 14 cm, necessitating a gap of ≈15 x 15 cm. A larger gap will not help in this mode of operation, but will increase the acceptance for pairs produced in the CLAS target as described in Section 2.4.

4. The counters must all be outside the photon beam or shielded from it, so that photons do not convert in the counters.

   No counter should be closer than ≈ 7.5 cm to the beam line.

5. The pair spectrometer must have reasonably flat acceptance for photons over the entire tagging range, $0.2\ E_0 \leq k \leq 0.95\ E_0$.

6. Only crude energy resolution is needed, but there should be several energy channels, with roughly equal singles rates, in order to avoid deadtime problems at high rate.

3.2 Dynamic Range

In first approximation, the energy spectrum of electrons and positrons produced by a photon beam of energy k is flat from 0 to k:

$$dN/dE_+ \approx dN/dE_- \approx \begin{cases} B & (0 < E_\pm < k) \\ 0 & (E_\pm > k) \end{cases} \qquad (5)$$

where B is a constant for a given k ($B \approx 7/9\ (x_{pair}/X_0)\ 1/k$, where x_{pair}/X_0 is the pair converter thickness in radiation lengths), and

$$E_+ + E_- = k\ . \qquad (6)$$

In order to implement Item 5 of the previous section, the pair spectrometer must detect electrons and positrons over a large "dynamic range", i.e. a large ratio of E_{max}/E_{min}. To detect both $e^\pm$ from a photon of $.2E_0$ with non-zero probability, E_{min} must be less than $.1E_0$. To detect a photon of $.95E_0$, E_{max} must be greater than $.475E_0$. Using these values of E_{min} and E_{max}, only symmetric pairs ($E_+ = E_-$) could be detected at the extreme photon energies. To detect photons of $.2E_0$ and $.95E_0$ with 50% efficiency, we need $E_{min} = .05E_0$ and $E_{max} = .75E_0$ (ratio 15:1), and 90% efficiency would require $E_{min} = .01E_0$ and $E_{max} = .95E_0$ (ratio 95:1).

3.3 Trajectories in the Pair Spectrometer Magnet

We assume a window-frame dipole magnet of approximate dimensions

L = field length	= 1.00 m
w = width	= 0.40 m
h = gap height	= 0.15 m
B_{max} = mag. field	= 1.00 T

These are approximately the dimensions of the old Brookhaven 18D36 magnet, which is typical of the kind of magnet we might hope to salvage for this project. The calculations below do not depend on the gap height h. The 1-T field may be conservative for a 15-cm gap, but will depend on the coil configuration and the available power supply.

We assume that electrons enter the field on the central axis and at zero angle. (The characteristic angle of the $e^\pm$ is $m_e/E_\pm$). It is useful to define the critical radius R_1 of the pair spectrometer as the radius of curvature of the least energetic electron which emerges from the other end of the magnet (just grazing the "corner"), and the critical energy E_1 as the corresponding energy. It is easy to show that, for a hard-edged uniform field,

$$R_1 = L^2/w + w/4 \tag{7}$$

$$E_1\ [\mathrm{MeV}] = 299.79\ B[\mathrm{T}]\ R[\mathrm{m}] \tag{8}$$

which, for the values above, gives $R_1 = 2.6$ m and $E_1 = 780$ MeV at $B = 1.0$ T. Trajectories for electrons at several multiples and submultiples of E_1 are shown in Figure 4. The accompanying positrons deflect in the opposite direction, so a pair event consists of a coincidence between two counters on opposite sides. Obtaining a large range of energies while satisfying Item 4 of Section 3.1 requires that counters be placed both inside and outside the magnet gap.

3.4 Pair Energy Acceptance

The lowest-energy electron which can be detected by counters inside the gap has radius of curvature $R \approx w/4 = 0.10$ m. The highest detectable electron energy depends on the size of the central aperture which must be kept free of counters and the maximum downstream distance at which counters can be placed. For the magnet specifications above, if we place the high-energy counters at 1.0 m from the end of the magnet and allow them to come no closer than 10 cm to the beam line, the range of energies is

$$E_{min} = E_1/26 = 30\ \mathrm{MeV}, \qquad E_{max} = 5.8\ E_1 = 4.5\ \mathrm{GeV}$$

so the 1.0 T field setting is perfect for a 4 GeV bremsstrahlung beam. Table 1 shows the fractional e^+e^- acceptance of the pair spectrometer, using Eq. (5) and assuming a narrow and perfectly centered photon beam, with $E_{min} = 40$ MeV and $E_{max} = 4$ GeV at $B = 1$ T. The acceptance at a given value of k/E_0 is independent of E_0 if the pair spectrometer field is scaled proportional to E_0.

3.5 Equal-Rate Counters

To allow the pair spectrometer to take data at high rate, the counters on either side should be segmented. This will have the additional benefit of providing some crude energy resolution for the pairs, which would provide a check on the treatment of multiple hits in the tagger.

For a given number of counters, the optimal division is one which produces equal event rates in the counters. The bremsstrahlung spectrum per incident electron of energy E_0 has the approximate form

$$dN/dk \approx \begin{cases} A/k & (k \le E_0) \\ 0 & (k > E_0) \end{cases} \qquad (9)$$

where the constant A is equal to the radiator thickness in radiation lengths ($A = x_r/X_0$). Using Equations (5) and (8), we can derive an approximate expression for the energy distribution of positrons (or electrons) produced by pair production by a bremsstrahlung beam:

$$dN/dE_+ \approx C\ (1/E_+ - 1/E_0) \qquad (10)$$

where $C = 7/9\ (x_r/X_0)(x_{pair}/X_0)$. This can be integrated to give the number of positrons (or electrons) whose energy is above a particular energy ϵ:

$$N(E_+>\epsilon) = C\ [\ \log(E_0/\epsilon) + \epsilon/E_0 - 1\ ] \qquad (11)$$

$$= C\ [\ y - \log(y) -1\ ] \qquad (y \equiv \epsilon/E_0)\ .$$

Table 2 shows two possible schemes in which the energy region from 0.05 E_1 to 5.13 E_1 (39 MeV to 4 GeV at B = 1.0 T) is divided into 5 and 10 counters per side with equal rates in each counter. Possible counter positions and the crossover trajectories are illustrated in Figure 5.

4. Conclusions and Questions

We have shown how the photon flux can be normalized using data from calibration runs taken with a total absorption shower counter and a pair spectrometer, and described how a suitable pair spectrometer can be constructed using a reasonable-sized magnet. The shower counter is a minor addition to the scope of the project, and is clearly necessary: we have no other way to determine channel efficiencies.

The pair spectrometer, while technically straightforward, is nonetheless a major piece of equipment. It may entail considerable expense for the power supply (comparable to the tagger magnet supply), detectors and electronics even if a surplus magnet can be obtained cheaply. The principal unanswered question concerning the pair spectrometer is: is it worth it?

As discussed above, the pair spectrometer serves two distinct functions:

1) testing the deadtime corrections in the absolute channel normalization procedure.

2) providing a relative luminosity monitor during the CLAS data runs.

The first of these seems hardly to justify a ≈$100K expenditure, at least in the initial configuration. The rate corrections are presumably calculable from pulse widths and electronics specifications, and can be measured to some degree by running at intermediate rates. It may be, then, that the more important justification for the pair spectrometer is in its second role, as a relative luminosity monitor, for which it is far from an optimal design because of its large distance from the CLAS. There has been very little discussion of the necessity for the luminosity monitor, or the possibility of generating equivalent information in another way. We should review such possibilities before committing any major resources to the development of the pair spectrometer.

Table 1. Fractional geometrical pair acceptance of the pair spectrometer versus photon energy k for two different field settings. The e^+e^- acceptance is equal to
$1 - 2E_{min}/k - 2[1-\mathrm{Min}\{1, E_{max}/k\}]$

	B = 1.00 T E_1 = 780 MeV E_{min} = 40 MeV E_{max} = 4000 MeV			B = 0.25 T E_1 = 195 MeV E_{min} = 10 MeV E_{max} = 1000 MeV		
k (MeV)	E_{min}/k	E_{max}/k	e^+e^- accept.	E_{min}/k	E_{max}/k	e^+e^- accept.
4000	.010	1.000	.980			
2000	.020	> 1	.960			
1600	.025	> 1	.950	.0063	0.625	.238
800	.050	> 1	.900	.0125	> 1	.975
400	.100	> 1	.800	.0250	> 1	.950
200	.200	> 1	.600	.0500	> 1	.900

Table 2. Boundaries of energy bins which divide the pair spectrometer into 5 or 10 pairs of counters with approximately equal counting rates. These values assume the geometry of Section 3.3 with E_{min} = .0513 E_1 and E_{max} = 5.13 E_1 (40 MeV and 4000 MeV at B = 1.0 T, where E_1 = 780 MeV).
Definitions: $y = \epsilon/E_0$, with E_0 = bremsstrahlung endpoint energy and ϵ = energy of $e^\pm$ which defines bin boundary; f(y) is a function which is proportional to the number of $e^\pm$ with energies greater than ϵ:

$$f(y) = (y - \log y - 1), \text{ where } y = \epsilon/E_0 \text{ (see Eq. (11))}$$

	10 equal-rate bins			5 equal-rate bins		
Bin	f(y)	$y=\epsilon/E_0$	ϵ/E_1	f(y)	$y=\epsilon/E_0$	ϵ/E_1
0	3.615	.0100	.051	3.615	.0100	.051
1	3.254	.0144	.074	2.892	.0208	.107
2	2.892	.0208	.107	2.170	.0439	.225
3	2.531	.0302	.155	1.446	.0953	.489
4	2.169	.0439	.225	.723	.2232	1.145
5	1.808	.0644	.330	.000	1.000	5.131
6	1.446	.0953	.489			
7	1.085	.1436	.737			
8	.723	.2232	1.145			
9	.362	.3716	1.907			
10	.000	1.000	5.131			

Data acquisition modes for calibrations

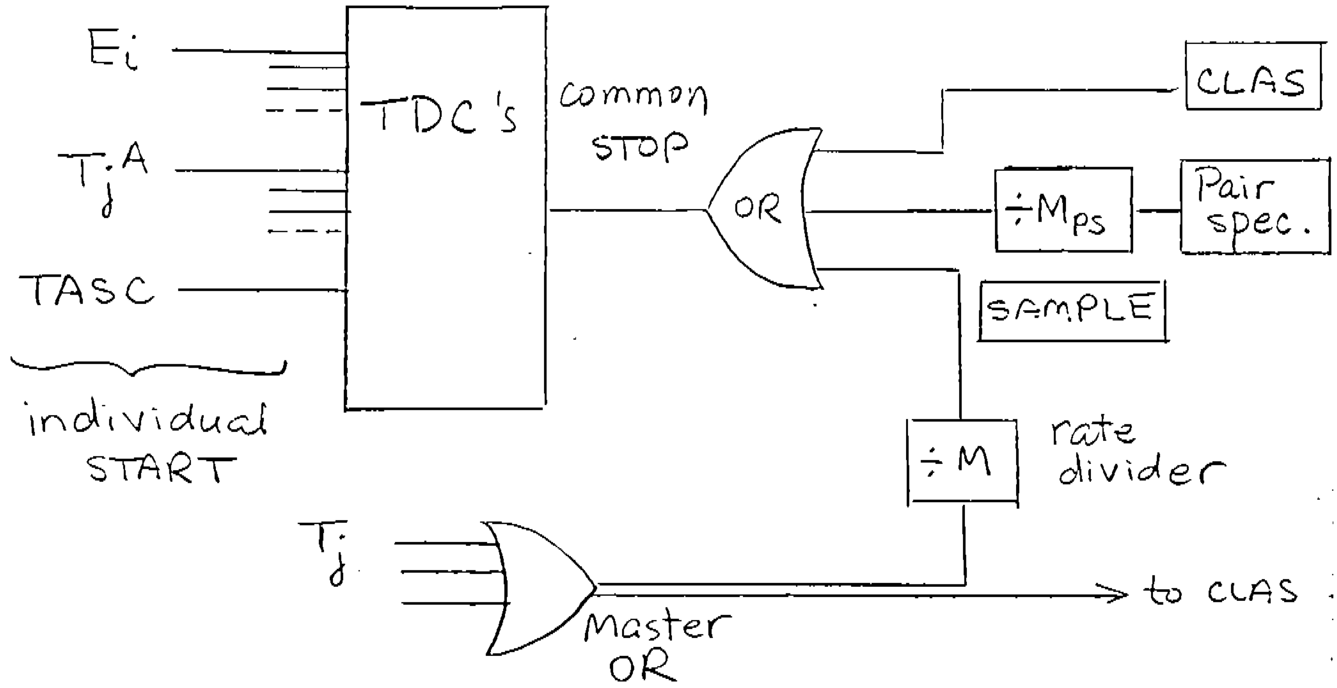

Run type	In trigger and TDC stop: CLAS	SAMPLE	Pair.Spec	Tag Rate
Data run	✓	$\div M$	$\div M_{ps}$	$\sim 10^7$
A TASC run		$\div 1$ (or $\div M$)		$\sim 10^5$
B PS-low		$\div M$	$\div 1$ (or $\div M_{ps}$)	$\sim 10^5$
C PS-high		$\div M$	$\div M_{ps}$	$\sim 10^7$

Get a different spectrum for each trigger mode:

CLAS spectrum
SAMPLE spectrum
PS spectrum

Figure 1. Data acquisition modes for photon flux normalization.

Calculation of photon flux on target using T-counter scalers

\# of photons on target in bin i

$$n_i = \overbrace{N_j}^{\text{data run}} \times \overbrace{\frac{n_i^{TASC}(cal)}{N_j(cal)}}^{\text{TASC run}} \times \epsilon_{TASC_i} \times \eta_{DT_i}$$

scaler for counter T_j corresp. to E_i

$$\eta_{DT\,i} = \underbrace{\frac{n_i^{PS}(PS\text{-}high)}{N_j\,(PS\text{-}high)}}_{\text{high-rate PS run}} \div \underbrace{\frac{n_i^{PS}(PS\text{-}low)}{N_j\,(PS\text{-}low)}}_{\text{low-rate PS run}}$$

Figure 2. Photon flux normalization by Method 1.

Calculation of photon flux on target using SAMPLE spectrum

photons on target in bin i

$$n_i = \overbrace{M \; n_i^S}^{\text{data run}} \times \overbrace{\frac{n_i^{TASC}(\text{cal.})}{n_i\,(\text{cal.})}}^{\text{TASC run}} \times \epsilon_{TASC_i} \times \eta_{DT_i}$$

events with TASC hit

TASC efficiency

rate division

events in bin i of SAMPLE spectrum

all events

deadtime correction (see below)

$$\eta_{DT_i} = \underbrace{\frac{n_i^S\,(\text{PS-low})}{n_i^{PS}\,(\text{PS-low})}}_{\text{low-rate PS run}} \div \underbrace{\frac{n_i^S\,(\text{PS-high})}{n_i^{PS}\,(\text{PS-high})}}_{\text{high-rate PS run}}$$

events in bin i of PS spectrum

Figure 3. Photon flux normalization by Method 2.

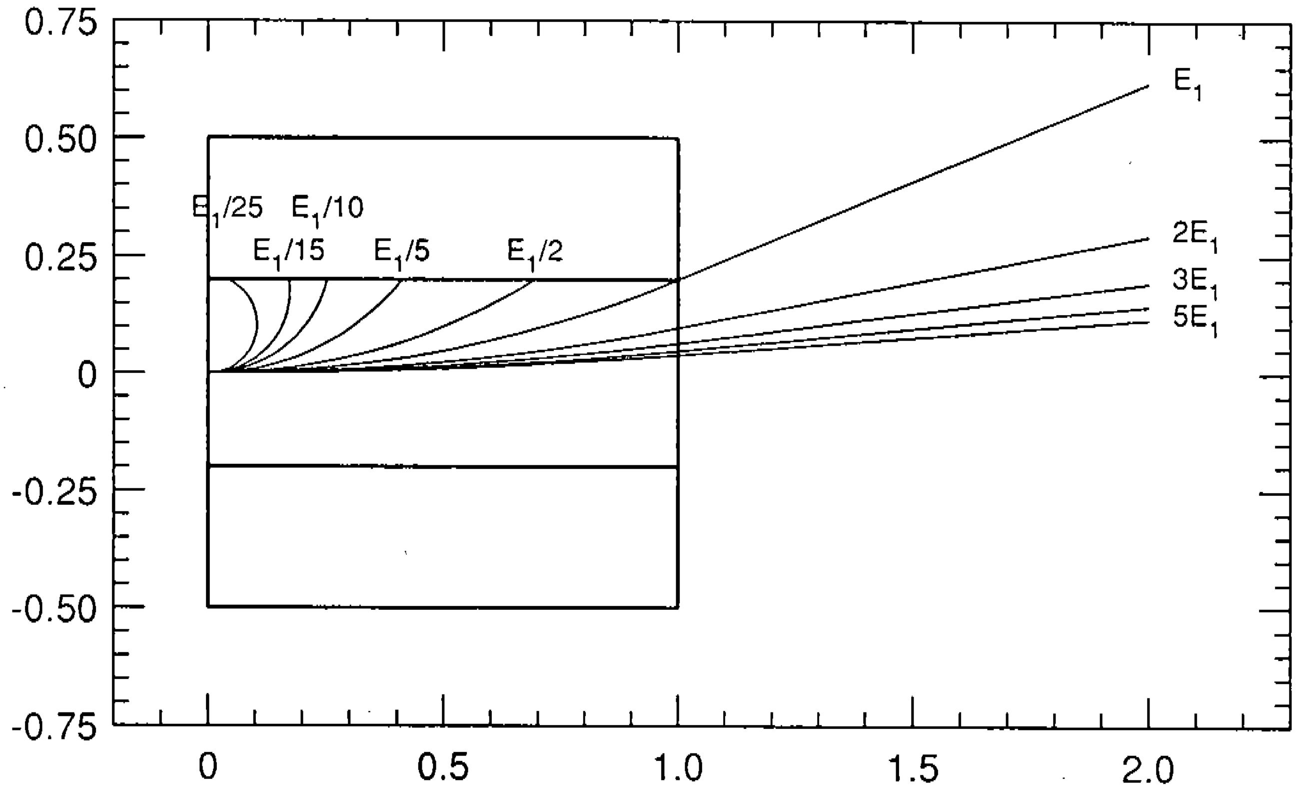

Figure 4. Typical electron trajectories in the pair spectrometer magnet whose geometry is described in Section 3.3. Each trajectory is labeled with its energy in units of the "corner" energy E_1 (E_1 = 780 MeV for B = 1.0 T).

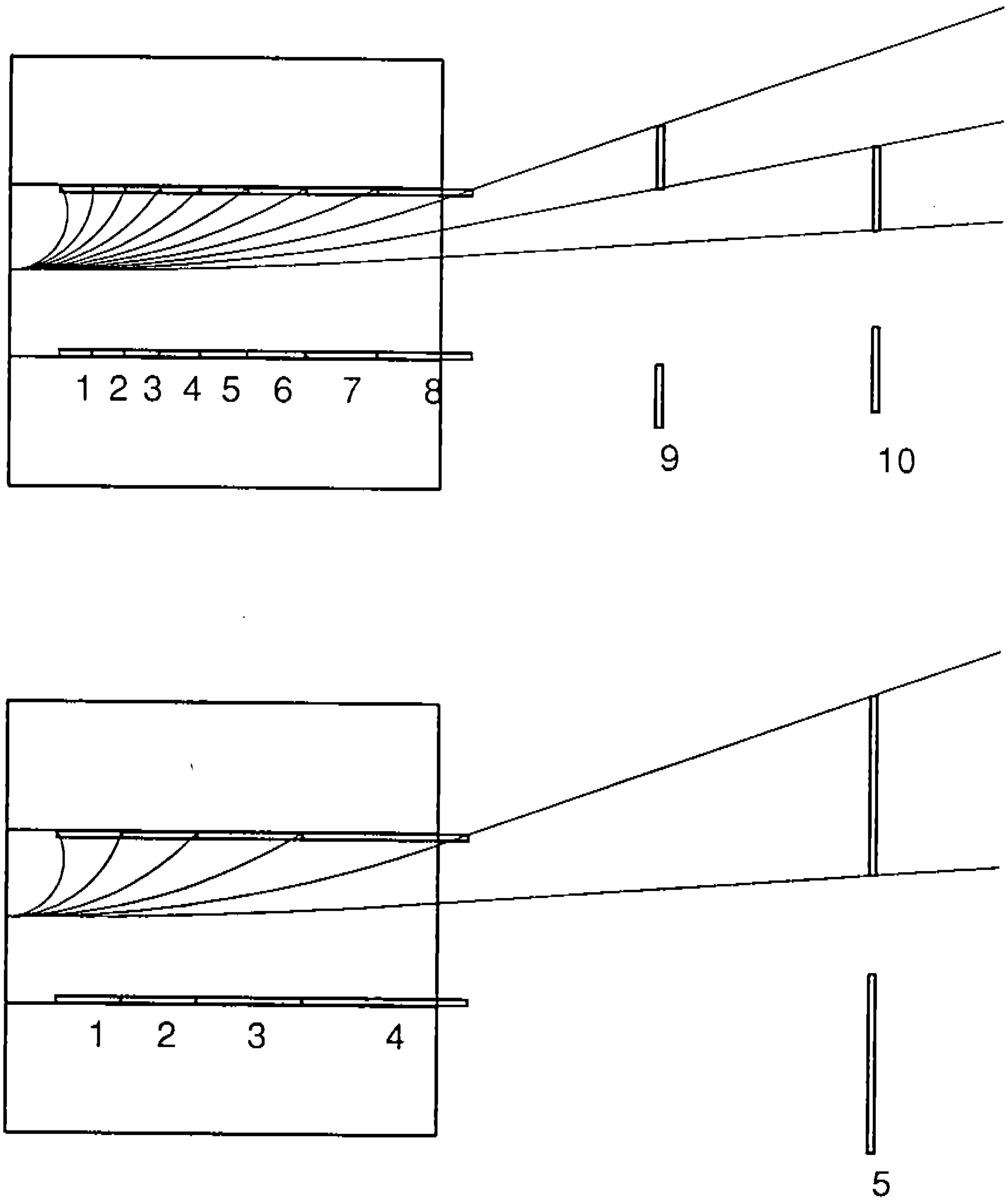

Figure 5. Positions of counters with approximately equal counting rates. The trajectories shown define the boundaries between the energy bins (see Table 2). (a) 5 equal-rate bins from $E = .0513\ E_0$ to $5.13\ E_0$ (40 MeV to 4 GeV at $B = 1.0$ T). (b) 10 equal-rate bins between the same limits.